

# Unmasking Stem-Specific Neutralizing Epitopes by Abolishing N-Linked Glycosylation Sites of Influenza Virus Hemagglutinin Proteins for Vaccine Design

Wen-Chun Liu,<sup>a</sup> Jia-Tsong Jan,<sup>b</sup> Yun-Ju Huang,<sup>a</sup> Ting-Hsuan Chen,<sup>a</sup> Suh-Chin Wu<sup>a,c</sup>

Institute of Biotechnology, National Tsing Hua University, Hsinchu, Taiwan<sup>a</sup>; Genomics Research Center, Academia Sinica, Taipei, Taiwan<sup>b</sup>; Department of Medical Science, National Tsing Hua University, Hsinchu, Taiwan<sup>c</sup>

## ABSTRACT

Influenza virus hemagglutinin (HA) protein consists of two components, i.e., a globular head region and a stem region that are folded within six disulfide bonds, plus several N-linked glycans that produce a homotrimeric complex structure. While N-linked glycosylation sites on the globular head are variable among different strains and different subtypes, N-linked glycosylation sites in the stem region are mostly well conserved among various influenza virus strains. Targeting highly conserved HA stem regions has been proposed as a useful strategy for designing universal influenza vaccines. Since the HA stem region is constituted by an HA1 N-terminal part and a full HA2 part, we expressed a series of recombinant HA mutant proteins with deleted N-linked glycosylation sites in the HA1 stem and HA2 stem regions of H5N1 and pH1N1 viruses. Unmasking N-glycans in the HA2 stem region (H5 N484A and H1 N503A) was found to elicit more potent neutralizing antibody titers against homologous, heterologous, and heterosubtypic viruses. Unmasking the HA2 stem N-glycans of H5HA but not H1HA resulted in more CR6261-like and FI6v3-like antibodies and also correlated with the increase of cell fusion inhibition activity in antisera. Only H5 N484A HA2 stem mutant protein immunization increased the numbers of antibody-secreting cells, germinal center B cells, and memory B cells targeting the stem helix A epitopes in splenocytes. Unmasking the HA2 stem N-glycans of H5HA mutant proteins showed a significantly improvement in the protection against homologous virus challenges but did so to a less degree for the protection against heterosubtypic pH1N1 virus challenges. These results may provide useful information for designing more effective influenza vaccines.

## IMPORTANCE

N-linked glycosylation sites in the stem regions of influenza virus hemagglutinin (HA) proteins are mostly well conserved among various influenza virus strains. Targeting highly conserved HA stem regions has been proposed as a useful strategy for designing universal influenza vaccines. Our studies indicate that unmasking the HA2 stem N-glycans of recombinant HA proteins from H5N1 and pH1N1 viruses induced more potent neutralizing antibody titers against homologous and heterosubtypic viruses. However, only immunization with the H5N1 HA2 stem mutant protein can refocus B antibody responses to the helix A epitope for inducing more CR6261-like/FI6v3-like and fusion inhibition antibodies in antisera, resulting in a significant improvement for the protection against lethal H5N1 virus challenges. These results may provide useful information for designing more effective influenza vaccines.

Members of the *Orthomyxoviridae* family, influenza A viruses are enveloped RNA viruses containing 8 negative-stranded RNA segments encoding 11 viral proteins, including the major surface proteins hemagglutinin (HA) and neuraminidase (NA) (1). Influenza A virus subtypes have been classified from H1 to H18 and N1 to N11 according to the antigenic properties of HA and NA (2). Beside the bat-associated H17 and H18, the subtypes (H1 to H16) can be divided into two groups, with H1, H2, H5, H6, H8, H9, H11, H12, H13, and H16 in group 1 and H3, H4, H7, H10, H14, and H15 in group 2 (3). Avian influenza viruses such as H5N1 and H7N9 have triggered epidemics resulting in significant human mortality rates (4). The continuing evolution of H5N1 and H7N9 avian influenza viruses has raised concerns about the potential for new human pandemics (5); accordingly, there is considerable research interest in developing more broadly protective vaccines against both seasonal and avian influenza viruses.

The HA protein, a major envelope glycoprotein, accounts for approximately 80% of all spikes in influenza virus virions. It is often used as antigen content for characterizing influenza vac-

cines. The HA protein consists of two components, i.e., a globular head region and a stem region that are folded within six disulfide bonds, plus several N-glycans that produce a homotrimeric complex structure (6). The acquisition of additional N-glycan modifications in the globular head has evolved as a strategy for seasonal H1N1 and H3N2 viruses to avoid human immune responses (7, 8). However, while N-linked glycosylation sites on the globular head are variable among different strains and different subtypes

Received 4 May 2016 Accepted 6 July 2016

Accepted manuscript posted online 20 July 2016

Citation Liu W-C, Jan J-T, Huang Y-J, Chen T-H, Wu S-C. 2016. Unmasking stem-specific neutralizing epitopes by abolishing N-linked glycosylation sites of influenza virus hemagglutinin proteins for vaccine design. *J Virol* 90:8496–8508. doi:10.1128/JVI.00880-16.

Editor: S. Perlman, University of Iowa

Address correspondence to Suh-Chin Wu, scwu@mx.nthu.edu.tw.

Copyright © 2016, American Society for Microbiology. All Rights Reserved.

(9), N-linked glycosylation sites in the stem region are mostly well conserved among various influenza virus strains (10). To date, several reports indicate that N-glycans in the HA1 stem regions of H7N1 and H5N1 viruses can affect the structural stability of less efficient HA cleavage, virus fusion, and virus replication (11, 12). It remains unclear whether N-glycans in the HA stem region affect anti-influenza virus immune responses, especially in terms of eliciting broadly neutralizing antibodies (bNAbs) and increasing protective immunity.

Targeting the highly conserved stem region has recently been proposed as a useful strategy for designing universal influenza vaccines (5, 13, 14). One approach uses the sequential immunization of chimeric HA DNA or protein containing a different heterotypic globular head but the same stem region for boosting stem-specific antibodies after repeated immunizations (15, 16). Another approach uses stem antigens that lack the globular head as soluble trimeric proteins (17), or perhaps incorporating them into ferritin nanoparticles for immunization purposes to elicit stem-specific antibodies (18). The third approach uses the glycan shielding on the variable regions in the HA globular head to redirect the immune responses to the more conserved HA stem region (19–21). Several reports also indicate that the HA stem-based influenza vaccines provide cross-subtype protection against diverse group 1 strains but not against diverse group 2 strains (15–18). In contrast, an H3 (group 2) stem-based HA vaccine is capable of inducing broadly neutralizing antistem antibodies and conferring broad protection against group 2 viruses in mice but not against diverse group 1 strains (22). To date, several bNAbs targeting HA stem epitopes have been obtained from human B cells, including CR6261 (23), F10 (24) (against most group 1 subtypes), and FI6v3 (25) (against group 1 and group 2 subtypes). The HA2 stem consists of five helical segments (A, C, D, G, and H), one B loop, and two strands (E and F) (26). All three stem-specific bNAbs are capable of binding to the helix A epitope in the F subdomain of the stem region (25). Some stem-specific bNAbs bind to HA via the  $V_H$  domain that originates from the human IGHV1-69 germ line gene with only a small number of somatic mutations (27). Allelic polymorphism (i.e., the rearrangement of VDJ gene segments) and somatic mutations are required for  $V_H$ 1-69 generation (28). Further, HA is capable of activating B cell receptors encoded with the germ line  $V_H$  sequence (IgM form), but only 2 mutations in the complementarity-determining region H1 and 5 mutations in the framework region 3 are required for the affinity maturation of precursor IgG, as well as for fully mature bNAb activity (29). However, it remains unclear how the stem helix A epitope contributes to bNAb development.

For this study, we expressed recombinant HA (rHA) proteins of H5N1 and pH1N1 viruses by deleting N-linked glycosylation sites located in the globular head, HA1 stem, or HA2 stem region. These stem glycan mutant rHA proteins were characterized using endoglycosidase and reacted with the globular head-specific and stem-specific (CR6261 and FI6v3) monoclonal antibodies (MAbs) for binding. These glycan mutant rHA proteins were used for mouse immunizations, and antisera were collected and analyzed for the elicitation of virus-neutralizing against homologous, heterologous, and heterosubtypic influenza viruses. The HA2 stem mutant proteins (H5 N484A and H1 N503A) were further characterized for the elicited immune responses of the cell fusion inhibition in antisera, the quantities of stem-specific CR6261-like or FI6v3-like antibodies, the numbers of stem helix A epitope-

specific B cell subsets in splenocytes, and protection against homologous and heterosubtypic lethal virus challenges.

## MATERIALS AND METHODS

**Recombinant H5HA and H1HA protein construction, expression, and purification.** Soluble H5HA (A/Thailand/KAN-1/2004) and pH1HA (A/Texas/05/2009) proteins were constructed using HA cDNA sequences and a Bac-to-Bac expression system as described in our previous studies (20, 30). Potential N-linked glycans were predicted using a NetNGlyc server. The N-X-S/T glycan motif was abrogated using site-directed mutagenesis. The HA stem mutant H5HA and pH1HA proteins were established by replacing asparagine (N) with alanine (A) at residues 10, 11, and 23 of H5HA (N<sup>10</sup>N<sup>11</sup>ST<sup>13</sup> replaced by A<sup>10</sup>A<sup>11</sup>ST<sup>13</sup> and N<sup>23</sup>VT<sup>25</sup> replaced by A<sup>23</sup>VT<sup>25</sup> and named N10A/N11A/N23A), replacing residue 484 of H5HA (N<sup>484</sup>GT<sup>486</sup> replaced by A<sup>484</sup>GT<sup>486</sup> and named N484A), replacing residues 32, 33, and 45 of pH1HA (N<sup>32</sup>N<sup>33</sup>ST<sup>35</sup> replaced by A<sup>32</sup>A<sup>33</sup>ST<sup>35</sup> and N<sup>45</sup>VT<sup>47</sup> replaced by A<sup>45</sup>VT<sup>47</sup> and named N32A/N33A/N45A), and replacing residue 503 of pH1HA (N<sup>503</sup>GT<sup>505</sup> replaced by A<sup>503</sup>GT<sup>505</sup> and named N503A). The above-described sequences were individually cloned into pFastBac expression vectors (Invitrogen). Next, wild-type (WT) and HA stem mutant proteins were produced using the Invitrogen Bac-to-Bac insect cell expression system according to the manufacturer's instructions. Briefly, Sf9 cells were infected with recombinant baculoviruses expressing the HA ectodomains of H5N1 and pH1N1 for 48 h prior to collecting supernatants for additional H5HA or pH1HA protein purification using nickel-chelated resin affinity chromatography (Tosoh). Wild-type and stem glycan mutant glycoprotein purities were confirmed by Coomassie blue staining. To characterize HA glycosylation patterns, wild-type and stem glycan mutant HA glycoproteins were treated with peptide-N-glycosidase F (PNGase F) (New England BioLabs) for 1.5 h at 37°C. HA glycosylation patterns were determined by Western blotting using anti-His horseradish peroxidase (HRP)-conjugated antibodies (Affymetrix).

**Mouse immunization.** Female 6- to 8-week-old BALB/c mice (5 per group) purchased from the Taiwan National Laboratory Animal Center were immunized intramuscularly (i.m.) twice with 20 µg of either WT or stem glycan mutant proteins of H5N1-rHA or pH1N1-rHA plus 10 µg CpG and 10% PELC emulsion over a 3-week interval (19, 20). Serum samples were collected at week 5, and the sera were inactivated at 56°C for 30 min to destroy complement prior to performing neutralization assays (both H5N1 pseudotyped particle [H5pp] assay and plaque reduction neutralization test [PRNT]); splenocytes were harvested and isolated at week 7. All animal studies were conducted in accordance with guidelines established by the Laboratory Animal Center of National Tsing Hua University (NTHU). Animal use protocols were reviewed and approved by the NTHU Institutional Animal Care and Use Committee (IACUC) (approval no. 10002). Mice that survived the immunization experiments were sacrificed using carbon dioxide (CO<sub>2</sub>) to ameliorate suffering.

**Viral challenges.** BALB/c mice were immunized with H5 WT, H5 N484A, H1 WT, or H1 N503A proteins plus CpG/PELC or phosphate-buffered saline (PBS). Three weeks following the second inoculations, all mice were intranasally (i.n.) challenged with 10 50% murine lethal doses (MLD<sub>50</sub>) of the H5N1 (NIBRG-14 and RG-14) or pH1N1 (A/California/07/2009 and CA/09) viruses. PBS-immunized mice were used as a mock control. Survival rates and body weights were monitored daily for 14 days. All mouse virus challenge procedures were reviewed and approved by the IACUC of Academia Sinica, Taiwan. According to IACUC guidelines, weight loss of 25% or more was established as an endpoint.

**Enzyme-linked immunosorbent assay (ELISA).** Individual wells in 96-well plates were coated with purified H5HA or pH1HA proteins (100 µl at 2 µg/ml), H5N1 (RG-14) inactivated virus (100 µl at 2 µg/ml), or pH1N1 (A/California/04/2009) virus (100 µl at 50 µg/ml), held overnight at 4°C, washed 3 times with 0.05% Tween 20 in PBS (PBST), and blocked with blocking buffer (1% bovine serum albumin [BSA] in PBS) for 1 h. Next, 100 µl of 2-fold serially diluted serum samples was added and held at room temperature (RT) for 1 h, followed by 3 additional washes with

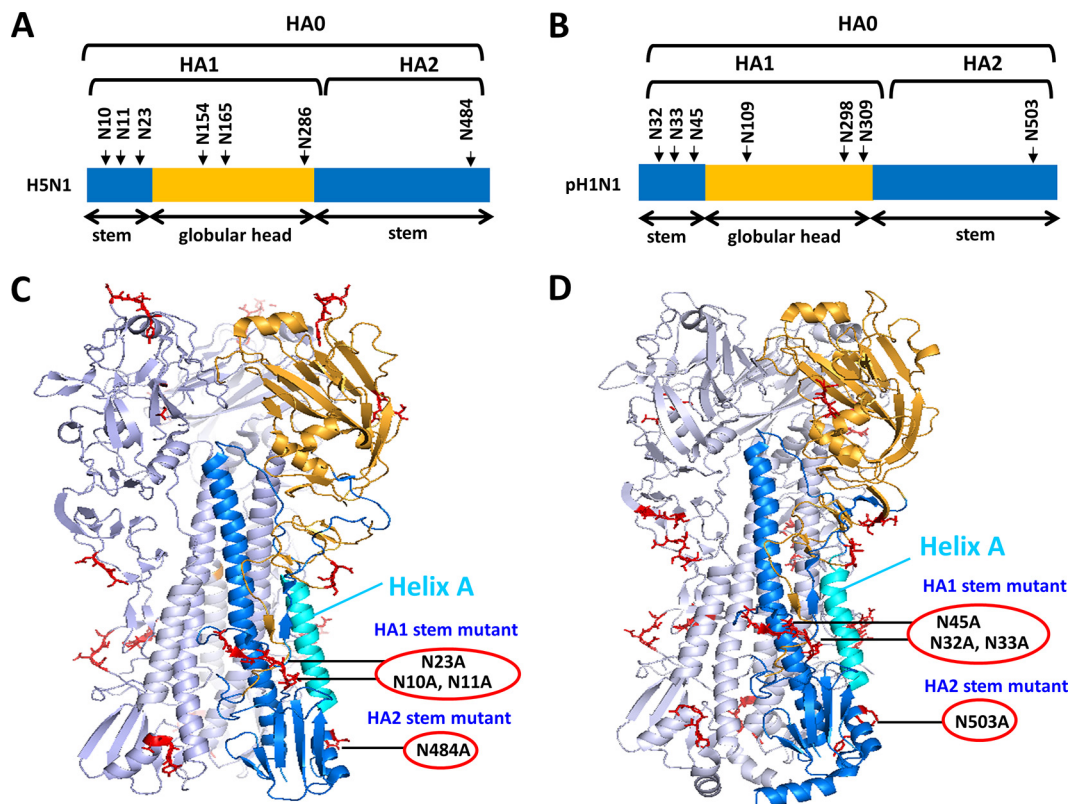


**FIG 1** Structural diagrams and unmasked-glycan rHA mutant glycoprotein designs. (A and B) Amino acid sequences for the rH5HA [A/Thailand/1(KAN1)/2004; GenBank accession number [AFF60787](#)] (A) and rH1HA [A/Texas/05/2009; GenBank accession number [ACP41934](#)] (B) ectodomains plus predicted N-glycan modification sites for both proteins. (C and D) Three-dimensional structural models for H5HA (C) and H1HA (D) (PyMol modeling software; PDB IDs 2IBX for H5HA and 3LZG for H1HA). Gray color, HA trimeric structure. Stem regions are highlighted in blue according to one of three identical monomers. Light blue, helix A motifs; orange, globular head; red, predicted N-linked glycan sites.

PBST. HRP-conjugated goat anti-mouse IgG antibodies (GeneTex Inc.) were added to each well, incubated for 1 h, and washed 3 times with PBST. Anti-HA IgG titers were determined by adding tetramethylbenzidine (TMB) substrate (BioLegend), holding for 15 min at RT, and stopping reactions with 2 N H<sub>2</sub>SO<sub>4</sub>. Endpoint titers were determined as the reciprocals of the most diluted sera concentrations giving a mean optical density (OD) above 0.2 at 450 nm.

**Lentivirus H5pp assay.** To neutralize antibodies against the H5N1 virus, neutralization titers were quantified as reduced luciferase expression levels using the lentivirus H5N1 pseudotyped particle (H5pp) assay as previously described (19, 20). Fifty microliters of H5pp at 100 50% tissue culture infective doses (TCID<sub>50</sub>) was incubated with 50  $\mu$ l of serially diluted antisera (1:10 starting dilution) for 1 h at 37°C, followed by the addition of 1.5  $\times$  10<sup>4</sup> MDCK cells per well. At 48 h postinfection, cells were lysed with Glo lysis buffer (Promega). Luciferase activity was measured by the addition of Neolite luciferase substrate (PerkinElmer). Fifty percent inhibitory concentrations (IC<sub>50</sub>s) were determined as the amounts of diluted sera required to obtain a 50% reduction in neutralizing activity compared to control wells containing the virus only.

**Plaque neutralization assay.** MDCK cells (8  $\times$  10<sup>5</sup>/well) were grown in 6-well plates, and on the following day cells were washed with PBS prior to the addition of 1 ml of 10-fold-diluted viruses containing 1.0  $\mu$ g/ml tosylsulfonyl phenylalanyl chloromethyl ketone (TPCK)-trypsin (Sigma-Aldrich) and incubated at 37°C for 1 h. After another washing with PBS, MDCK cells were overlaid with minimal essential medium alpha (MEM- $\alpha$ ) containing 0.5% agarose (Lonza) and held for 48 h, after which cells were fixed with 4% paraformaldehyde (PFA) and stained with 1% crystal violet prior to plaque counting per well. For PRNT assays, MDCK

cells were prepared as described above. The following day, 2-fold serially diluted immunized sera were mixed with equal volumes of 100 PFU/ml of pH1N1 (A/California/04/2009) or H3N2 (A/Udorn/307/1972) virus in MEM- $\alpha$  containing 1.0  $\mu$ g/ml trypsin-TPCK and held for 1 h at 37°C prior to performing plaque assay. Plaque counts and IC<sub>50</sub> values were calculated using PRISM v5.03 software.

**Protein absorption and antibody competition assays.** Two mutant HA proteins (H5  $\Delta$  stem protein and H1  $\Delta$  stem protein) were constructed by the introduction of N-glycans at the stem regions as previously reported (31). Protein absorption assays were performed using H5  $\Delta$  stem protein or H1  $\Delta$  stem protein to abrogate stem-binding antibodies (20, 31). Mouse serum was absorbed with 40  $\mu$ g/ml of H5  $\Delta$  stem protein- or H1  $\Delta$  stem protein-coupled Ni-nitrilotriacetic acid (NTA) beads and incubated overnight at 4°C. Absorbed sera were used with ELISA plates coated with H5HA or pH1HA proteins to measure IgG titers as previously described. For the CR6261 and FI6v3 MAb competition assays, ELISA plates precoated with H5HA or pH1HA were cocultured with mixtures of 2-fold-diluted MAb CR6261 or FI6v3 (starting from 10  $\mu$ g/ml) and  $\Delta$  stem preabsorbed antisera for 1 h. ELISAs were used to measure IgG titers.

**Quantitative cell-cell fusion assay.** Fusion inhibition activity against pH1N1 and H5N1 viruses were determined by luciferase-based cell-cell fusion assays as previously described (32, 33). In brief, effector cells (2  $\times$  10<sup>4</sup> 293T cells in 96-well plates) and target cells (9  $\times$  10<sup>5</sup> 293T cells in 6-well plates) were incubated overnight, followed by the transfection of pcDNA3.1-H5HA (KAN-1) or pcDNA3.1-pH1HA (RG-121) and pCAGT7pol plasmids into effector cells using TurboFect reagent (Thermo). Trypsin-TPCK (1.0  $\mu$ g/ml) was added into pcDNA3.1-pH1HA (RG-121)-transfected 293T effector cells for facilitating HA0



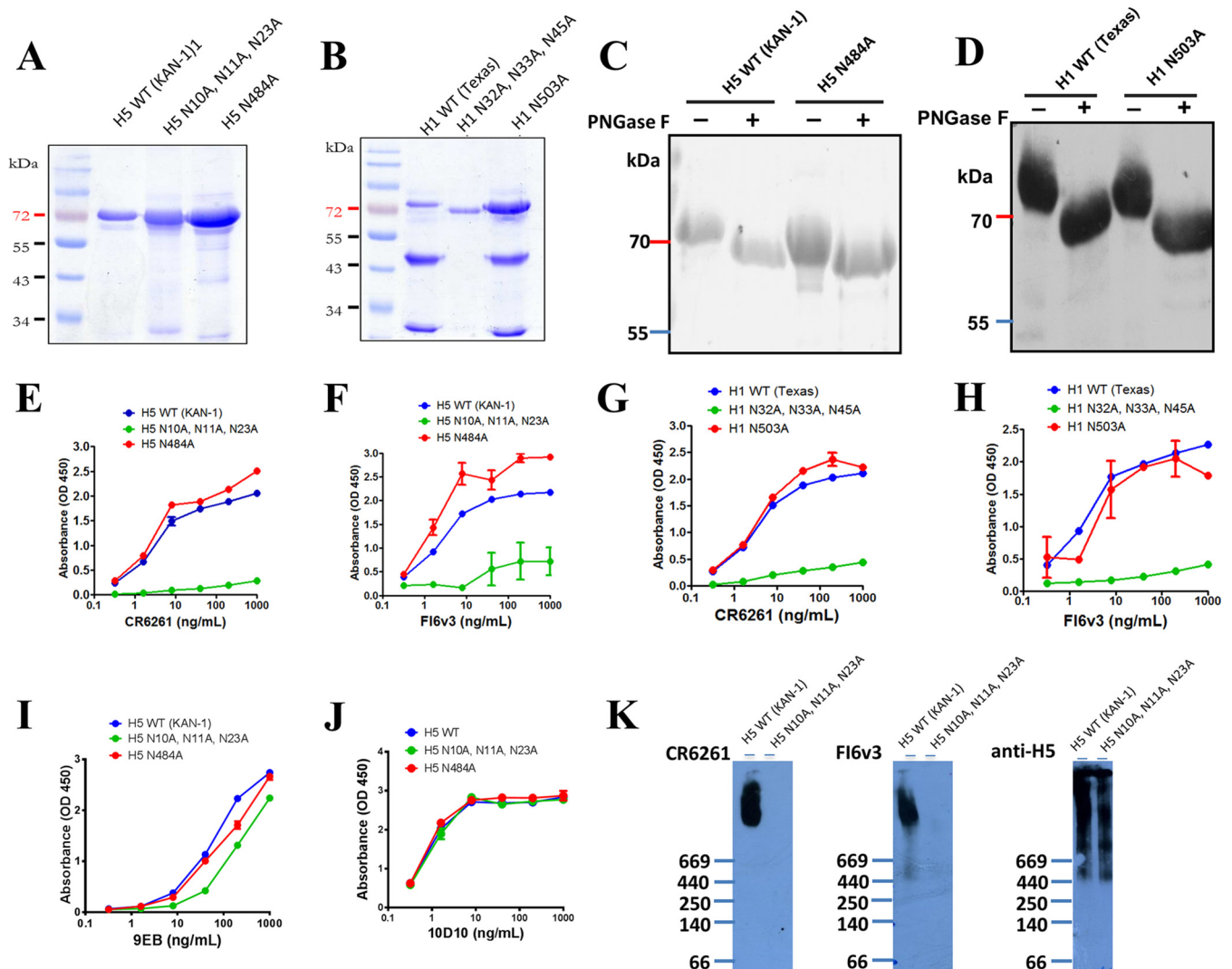


**FIG 2** Glycan-unmasked rHA mutant glycoprotein characterization. (A and B) SDS-polyacrylamide gels with Coomassie blue staining for the expressed WT and glycan-unmasked (HA1 stem and HA2 stem) H5HA (A) and pH1HA (B) WT and mutant proteins. (C and D) Western blotting for the expressed WT and HA2 stem mutant proteins of H5HA (C) and pH1HA (D) without and with PNGase F treatments in SDS-polyacrylamide gels. (E to J) ELISA binding assays were used to characterize the WT and mutant protein bindings with CR6261 (E and G), Fl6v3 (F and H), 9E8 (I), or 10D10 (J) MAbs. (K) Western blotting for the H5HA WT and triple mutant reacted with CR6261 and Fl6v3 in native polyacrylamide gels.

cleavage. Both pHRL-TK (Promega) and pT7EMCVLuc plasmids were cotransfected into target cells. The pT7EMCVLuc plasmid contains a firefly luciferase coding sequence under the control of the *Escherichia coli* T7 promoter, and the pHRL-TK plasmid has a sea pansy *Renilla* luciferase coding sequence under the control of the thymidine kinase (TK) promoter. *Renilla* luciferase expression was used as an internal control for transfection efficiency. After 48 h of transfection, target cells were detached from wells and added to effector cells. Next, diluted serum obtained from WT or HA2 stem mutant immunization in MEM- $\alpha$  containing 1.0  $\mu$ g/ml trypsin-TPCK was mixed with target and effector cells for 1 h at 37°C. Cocultures were washed and incubated with low-pH fusion buffer (PBS, pH 4.9) for 5 min at 37°C. Cells were returned to the standard growth medium for 7 h of incubation. Firefly and *Renilla* luciferase activities were determined using a dual-luciferase reporter assay system (Promega) and measured in terms of relative luminescence units (RLU) using a Victor 2 plate reader (PerkinElmer). The *Renilla* luciferase activity of the negative control (pT7EMCVLuc/pRL-TK-transfected 293T cells alone) was defined as 1. RLU were calculated as normalized firefly luciferase value/normalized *Renilla* luciferase value.

**HA-specific-antibody-secreting B cells (ASCs).** Splenocytes were collected from each group of HA2 stem mutant rHA-immunized or PBS-immunized mice at 4 weeks following their second inoculations. Multi-screen 96-well filtration plates (Millipore) were coated with H5HA or pH1HA proteins (1  $\mu$ g/well) and incubated overnight at 4°C. Plates were washed and blocked with RPMI containing 10% fetal bovine serum (FBS) for 1 h at 37°C. Splenocytes ( $1 \times 10^6$ ) were added to individual plates, stimulated with H5 or H1 helix A or nonrelated stem<sub>518–526</sub> peptides, and incubated for 48 h at 37°C. After 3 washes with PBST, HRP-conjugated anti-mouse IgG antibodies were added to each well and held for 2 h at RT. After 3 PBST and 2 PBS washes, 3-amino-9-ethylcarbazole (AEC) substrate (Sigma-Aldrich) was added to each plate and held at RT for 30 to 60 min prior to the reactions being stopped with double-distilled water (ddH<sub>2</sub>O). Immunospots for each immunized group were determined using an enzyme-linked immunosorbent spot (ELISPOT) plate reader (CTL, Inc.).

**GC and memory B cell analyses using flow cytometry.** Flow cytometry analyses (BD Accuri C6) were performed to determine the proliferation of germinal center (GC) B cells and memory B cells as previously

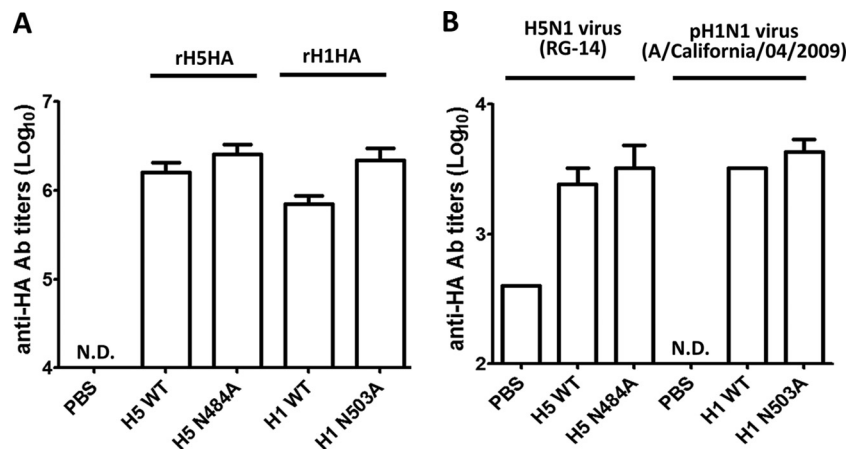


**FIG 3** Total IgG titers elicited by HA2 stem mutant proteins of rH5HAs and rH1HAs. Serum samples were collected from mice immunized with PBS or WT or HA2 stem mutant proteins and measured for HA-specific total IgG titers using ELISA. Shown are data for total IgG titers against rH5HA or rH1HA proteins (A) or H5N1 (RG-14) inactivated viruses or pH1N1 viruses (B) (0.2 endpoint). Data are expressed as means  $\pm$  standard deviations (SD). N.D., nondetectable.

described (34). In brief,  $1 \times 10^6$  splenocytes per well were stimulated by 20  $\mu$ g/ml of helix A (H5 or H1) or nonrelated stem<sub>518–526</sub> peptides for 48 h. Cells were harvested and fixed with 1% formaldehyde for 30 min at 4°C. Stimulated splenocytes were suspended in staining buffer (2% FBS and 0.01% NaN<sub>3</sub> dissolved in PBS), simultaneously stained with anti-IgG1–fluorescein isothiocyanate (FITC) (BioLegend) and anti-CD38–phyco-

erythrin (PE) (e-Bioscience) antibodies, and held for another 30 min at 4°C. The IgG1<sup>+</sup> CD38<sup>−</sup> cells (GC B cells) and IgG1<sup>+</sup> CD38<sup>+</sup> cells (memory B cells) were gated and analyzed using Accuri C6 software.

**Statistical analyses.** Most of the results were analyzed using one-way analysis of variance (ANOVA) or two-tailed Student *t* tests (GraphPad Prism v5.03). The survival curves were compared by using the Mantel-

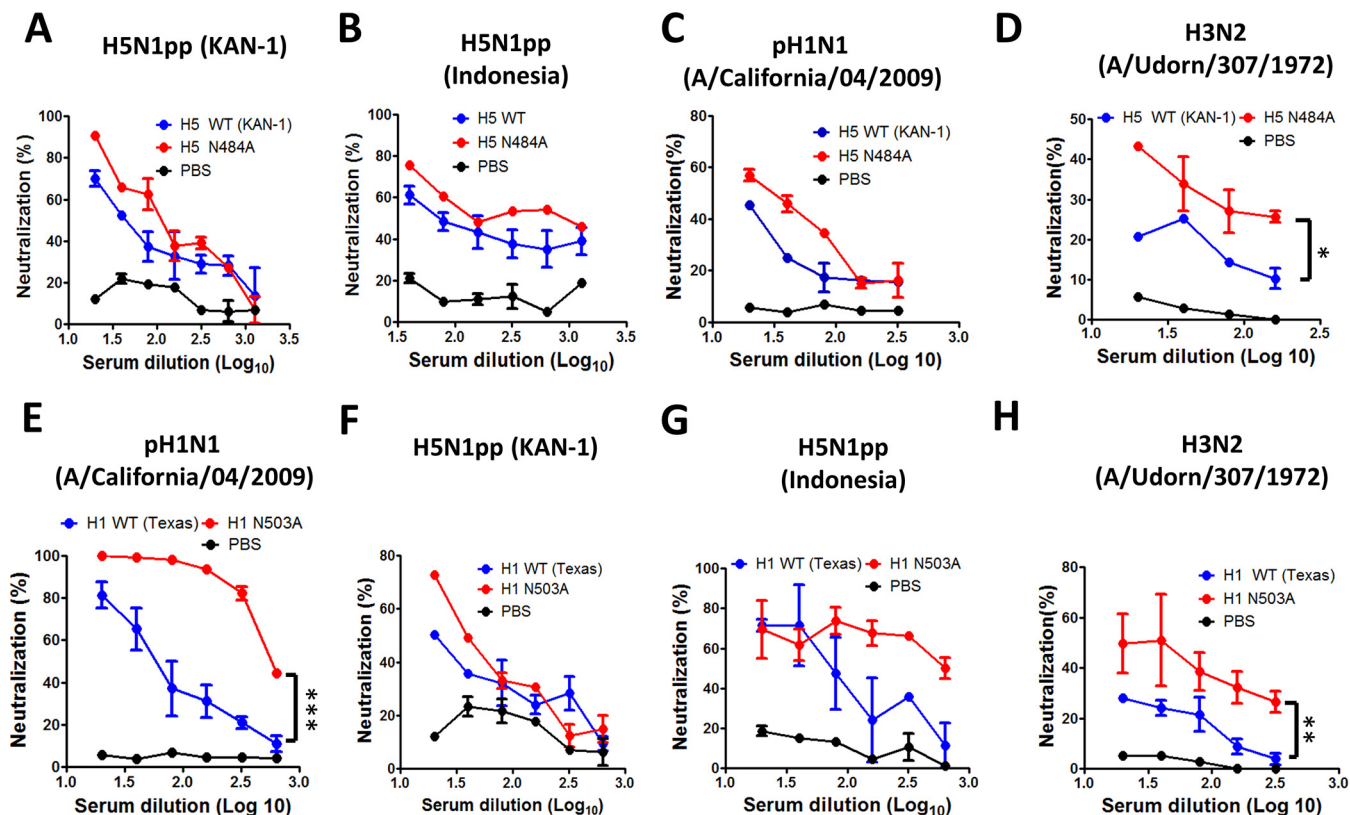


**FIG 4** Virus neutralization curves from immunizations with rH5HAs and rH1HAs HA2 stem mutants against different virus strains. Serum samples obtained from H5 WT-, H5 N484A-, H1 WT-, H1 N503A-, or PBS-immunized groups were 2-fold serially diluted. Neutralizing strengths against clade 1 (KAN-1) H5N1-pseudotyped particles (H5pp) (A and F) and clade 2.1.3.2 H5pp (Indonesia) (B and G) were determined by H5pp luciferase activity detection. Neutralizing strengths against pH1N1 (A/California/04/2009) (C and E) and H3N2 (A/Udorn/307/1972) (D and H) viruses were determined using PRNT assays. Statistical analysis was performed using one-way ANOVA. \*,  $P < 0.05$ ; \*\*,  $P < 0.01$ ; \*\*\*,  $P < 0.001$ .

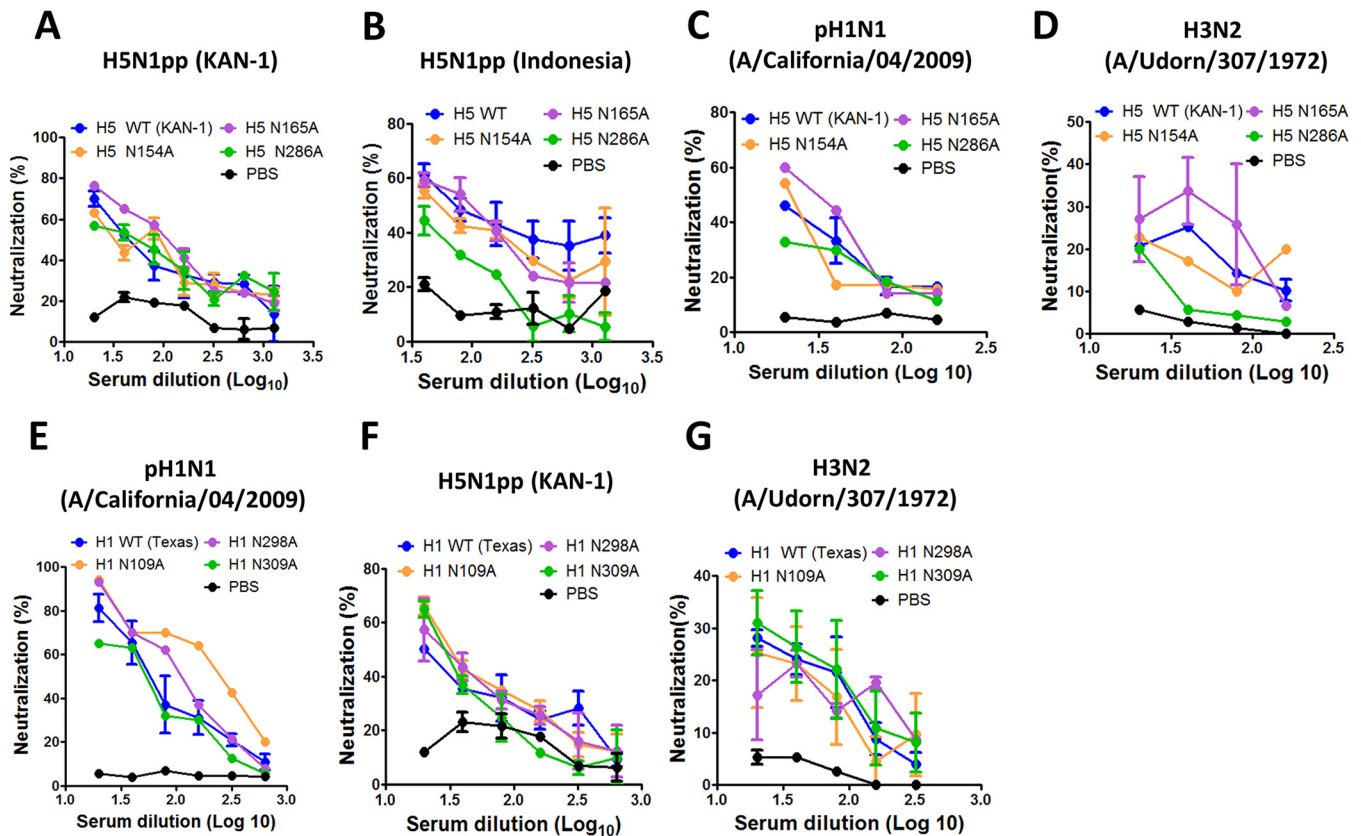


FIG 5 Virus neutralization curves from immunizations with rH5HAs and rH1HAs HA1 globular head mutants against homologous and heterosubtypic viruses. Serum samples obtained from H5 WT-, H5 N154A-, H5 N165A-, H5 N286A-, H1 WT-, H1 N109A-, H1 N298A-, H1 N309A-, or PBS-immunized groups were 2-fold serially diluted. Neutralizing strengths against H5pp of clade 1 (KAN-1) (A and F) and clade 2.1.3.2 H5pp (Indonesia) (B) strains were determined using H5pp luciferase activity assays. Neutralizing strengths against pH1N1 (A/California/04/2009) (C and E) and H3N2 (A/Udorn/307/1972) (D and G) viruses were determined using PRNT assays. Statistical analysis was performed using one-way ANOVA.

Cox log rank test followed by pairwise comparison with the Gehan-Breslow-Wilcoxon test. Statistical significance in all figures is expressed as follows: \*,  $P < 0.05$ ; \*\*,  $P < 0.01$ ; and \*\*\*,  $P < 0.001$ . All experiments were performed at least two times each.

## RESULTS

**Stem glycan mutant rHA protein expression and characterization.** The influenza virus HA stem region, which has a trimeric structure consisting of an HA1 N-terminal part and full HA2 part, contains several potential sites for the addition of N-glycans. Based on the HA sequences of H5N1 [A/Thailand/1(KAN-1)/2004; GenBank accession number [AFF60787](#)] and pH1N1 [A/Texas/05/2009; GenBank accession number [ACP41934](#)] and their predicted three-dimensional (3D) structures as previously described by others (11, 12), we found four potential H5HA N-glycosylation sites, with three located in the HA1 stem region (positions N10, N11, and N23) and one in the HA2 stem region (N484) (Fig. 1A). We also located four potential pH1HA N-glycosylation sites, three in the HA1 stem region (positions N32, N33, and N45) and one in the HA2 stem region (N503) (Fig. 1B). To unmask site-specific N-glycans in the HA stem region, both HA1 stem and HA2 stem mutants of H5 and H1 proteins were expressed by replacing asparagine (N) with alanine (A) at the N-linked glycosylation sites, with an N-X-S/T motif noted in the HA1 (H5 N10A/N11A/N23A and H1 N32A/N33A/N45A) and HA2 (H5 N484A

and H1 N503A) stem domains (Fig. 1C and D). Six wild-type (WT) and stem glycan mutant rHA proteins (H5 WT, H5 N10A/N11A/N23A, H5 N484A, H1 WT, H1 N32A/N33A/N45A, and H1 N503A) were obtained from Sf9 insect cells infected with recombinant baculoviruses, harvested from culture supernatants, purified using Ni chelation affinity chromatography, and analyzed using SDS-PAGE with Coomassie blue staining (Fig. 2A and B). H5 N484A and H1 N503A both exhibited reduced molecular weights in SDS-PAGE gels compared to the H5 and H1 WT proteins, thus confirming the removal of the HA2 stem N-glycans via the disruption of specific N-linked glycosylation sites (Fig. 2C and D). Following PNGase F treatment, these WT and mutant proteins shifted to the same molecular weights as with the removal of overall N-glycans of HA molecules (Fig. 2C and D). Two HA stem-specific bNAbs, CR6261 (group 1) and FI6v3 (groups 1 and 2), were used for reactions with purified WT and stem glycan mutant rHAs, as shown in the ELISA binding curves presented as Fig. 2E to H. HA2 stem mutant protein bindings (H5 N484A and H1 N503A) were similar to those for H5 and H1 WT proteins. In comparison, HA1 stem mutant protein bindings (H5 N10A/N11A/N23A and H1 N32A/N33A/N45A) were significantly reduced (Fig. 2E to H). We also used two H5HA globular head-specific MAbs (9E8 and 10D10) reported previously (20) to confirm whether these mutant rHA proteins were correctly



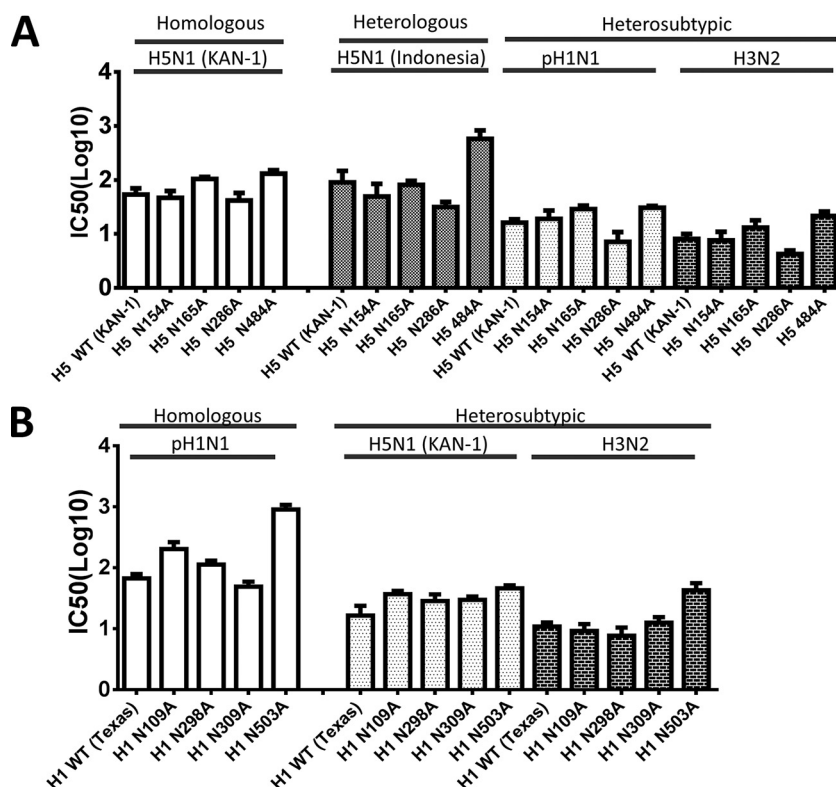


**FIG 6** IC<sub>50</sub> values of the globular head or the HA2 stem mutant groups against H5N1, pH1N1, and H3N2 virus strains. The corresponding IC<sub>50</sub> values were calculated (either interpolated or extrapolated) from the serum neutralization curves of the globular head and stem 2 mutant immunized groups against H5N1 clade 1 (KAN-1) and H5N1 clade 2.1.3.2 (Indonesia), pH1N1 (A/California/04/2009), and H3N2 (A/Udorn/307/1972) viruses.

folded. Our results showed that the binding curves of both HA1 stem and HA2 stem mutants were similar to those of the H5WT proteins (Fig. 2I and J). The loss of binding of the triple mutant (H5 N10A/N11A/N23A) to FI6V3 and CR6261 bNAbs was confirmed in native polyacrylamide gels (Fig. 2K). Taken together, these results indicate that only the two HA2 stem mutant proteins (H5 N484A and H1 N503A), with stem N-glycans removed by site-directed mutagenesis, retained their binding capabilities with the stem-specific bNAbs CR6261 and FI6v3.

**HA-specific IgG and virus-neutralizing antibodies elicited by HA2 stem mutant protein immunization.** To further characterize HA immunogenicity affected by the loss of stem N-glycans, groups of 6- to 8-week-old female BALB/c mice were i.m. immunized with two doses of 20 µg WT or HA2 stem mutant proteins (H5 WT, H5 N484A, H1 WT, or H1 N503A) formulated with PELC/CpG adjuvant over a 3-week interval. Antisera were collected at 2 weeks following the second immunizations. Our results show that the HA2 stem mutant proteins (H5 N484A and H1 N503A) elicited HA-specific IgG titers similar to those for the WT proteins, as measured by ELISAs using rH5HA and rH1HA proteins (Fig. 3A) or H5N1 RG14 (inactivated) and pH1N1 (A/California/04/2009) viruses (Fig. 3B). Serum neutralization curves and their corresponding 50% inhibition concentrations (IC<sub>50</sub>s) were obtained using H5N1 pseudotyped particle (H5pp) and plaque reduction assays for the pH1N1 and H3N2 viruses. The results indicate dose dependency for the serum neutralization curves against the H5N1 (KAN-1, Indonesia), pH1N1 (A/California/04/2009), and H3N2 (A/Udorn/307/1972) viruses

(Fig. 4). The neutralization curves for immunizations with the HA2 stem mutant proteins (H5 N484A and H1 N503A) were more effective than those elicited by immunizations with the WT (nonmutant) proteins (H5 WT and H1 WT), showing statistical significance for the H5 N484A antiserum against H3N2 virus (Fig. 4D) and the H1 N503A antisera against pH1N1 viruses (Fig. 4E) and H3N2 viruses (Fig. 4H). No dose-dependent neutralization activities were shown for the antisera obtained from the PBS-immunized groups. Additionally, we also obtained the H5 and H1 mutant proteins by the removal of three potential N-linked glycosylation sites located in the globular head regions (H5HA residues 154, 165, and 286 and pH1N1 residues 109, 298, and 309), whereas only the N-glycan removal of H5HA residue 286 was recently reported (12). Antisera obtained from immunizations using the globular head mutant proteins H5 N154A, H5 N165A, H5 N286A, H1 N109A, H1 N298A, and H1 N309A were also measured against the H5N1, pH1N1, and H3N2 viruses. No significant improvements in their neutralization curves were observed for these globular head mutant proteins compared to those for the WT proteins (Fig. 5). The corresponding IC<sub>50</sub> values calculated from these neutralization curves are summarized in Fig. 6. The IC<sub>50</sub> values of the H5 N484A groups were higher than those of the H5 WT groups against the homologous H5N1 virus (KAN-1, clade 1), the heterologous H5N1 virus (Indonesia, clade 2.1.3.2), and the heterosubtypic H3N2 virus (Fig. 6A). The IC<sub>50</sub> values of the globular head N-glycan mutants (H5 N154A, H5 N165A, and N286A) were either similar or lower to those of the H5 WT groups (Fig. 6A). The H1 N503A group had an increased IC<sub>50</sub> value against the homol-

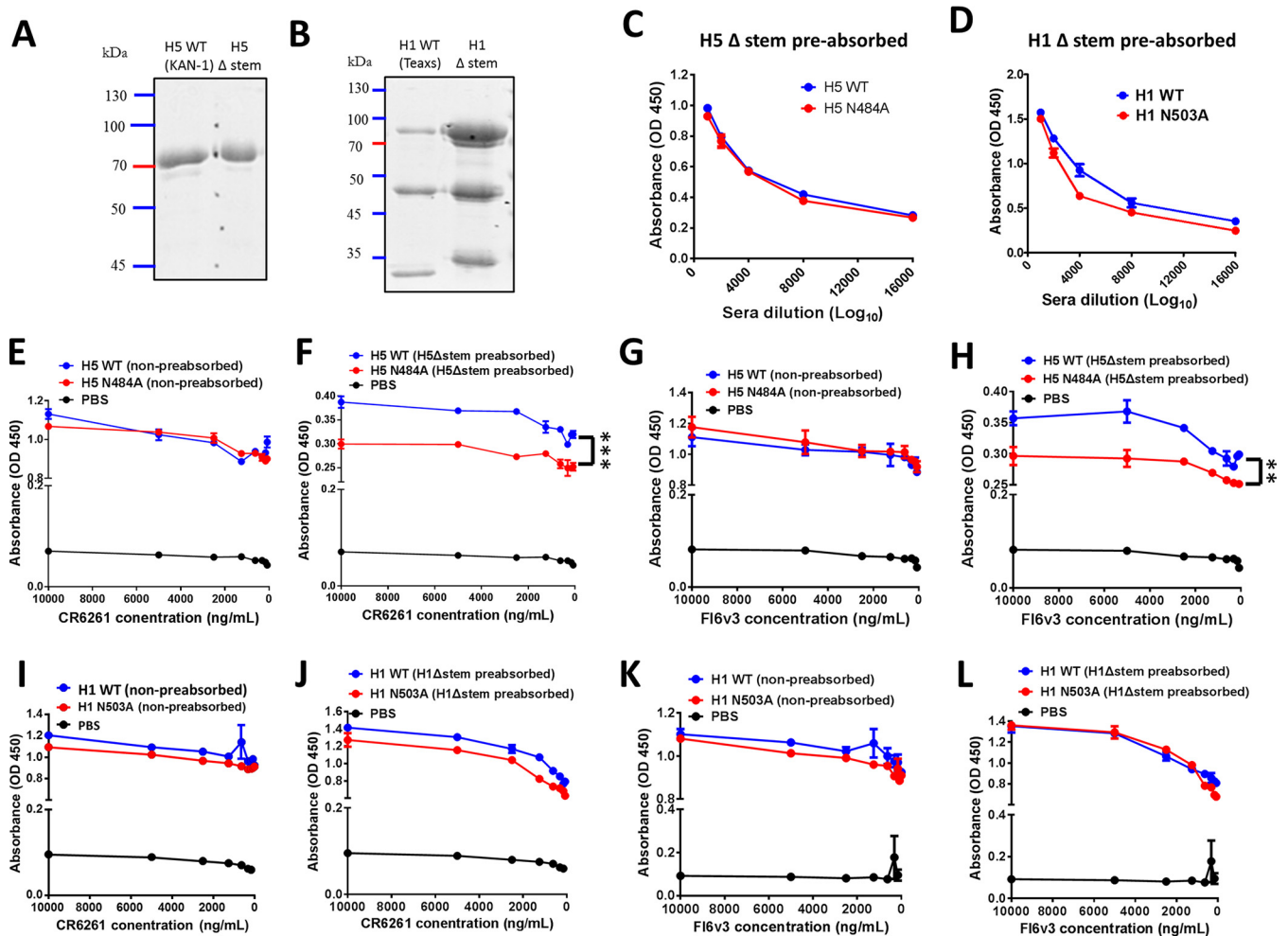


FIG 7 Mapping of stem-specific antibodies elicited by rH5HAs and rH1HAs HA2 stem mutants. (A and B) H5HA and H1HA mutant proteins containing an additional N-glycan, H5  $\Delta$  stem protein (A) or H1  $\Delta$  stem protein (B), for mapping stem-specific antibodies were constructed and characterized by SDS-PAGE. Serially diluted sera collected from the WT or HA2 stem mutant protein-immunized mice were separately absorbed with H5  $\Delta$  stem or H1  $\Delta$  stem proteins. (C and D) ELISAs were used to determine the remaining IgG titers. (E to K) Stem-specific Abs elicited by the HA2 stem mutant H5 N484A or H1 N503A were identified using competitive ELISAs. The serum samples nonpreabsorbed (E, G, I, and K) or preabsorbed with H5  $\Delta$  stem protein (F and H) or H1  $\Delta$  stem protein (J and L) were mixed with 2-fold serially diluted bAbs (CR6261 or FI6v3) and added to plates precoated with rH5HA or rH1HA proteins. HA-specific IgG titers were measured using ELISAs. OD values at 450 nm induced by WT and HA2 stem mutant proteins were plotted. Integrated data are expressed as mean  $\pm$  SD. Statistical analysis was performed using one-way ANOVA. \*,  $P < 0.05$ ; \*\*,  $P < 0.01$ . \*\*\*,  $P < 0.001$ .

ogous pH1N1 virus and to a less degree against the heterosubtypic H3N2 virus (Fig. 6B). Other globular head mutants (H1 N109A, H1 N298A, and H1 N309A) had IC<sub>50</sub> values similar to those of the H1 WT group (Fig. 6B). Therefore, unmasking N-glycans in the HA2 stem region (H5 N484A and H1 N503A) elicited more potent neutralizing antibodies against homologous, heterologous, and heterosubtypic influenza viruses.

**Mapping stem-specific antibodies elicited by HA2 stem mutant protein immunizations.** Introduction of N-glycans into midstem helix A in stem mutant proteins is a method previously reported for mapping stem-specific antibodies (31). We adapted this strategy and constructed H5HA and H1HA mutant proteins containing an additional N-glycan at residue I375N and a G377T change for the H5HA stem mutant (H5  $\Delta$  stem protein) and residue I394N and E396T changes for the H1HA stem mutant (H1  $\Delta$  stem protein) (Fig. 7A and B). Immune sera from either H5 WT and H5 N484A or H1 WT and H1 N503A were untreated or

treated with H5  $\Delta$  stem or H1  $\Delta$  stem proteins bound to Ni beads for purposes of preabsorbing non-stem-specific antibodies. We then used ELISAs to measure stem-specific antibodies bound to rH5HA or rH1HA proteins. Our results indicate the dose-dependent presence of stem-specific antibodies in all groups of antisera, but no significant differences in stem-specific antibodies were noted following immunizations with H5 WT and H5 N484A or H1 WT and H1 N503A (Fig. 7C and D). To further characterize the broadly neutralizing epitopes, competition assays were performed using two stem-specific bAbs, CR6261 and FI6v3. Antisera either were not preabsorbed or were preabsorbed with H5  $\Delta$  stem or H1  $\Delta$  stem proteins prior to competition with different concentrations of MAb CR6261 or FI6v3. According to the ELISA results, the nonpreabsorbed sera from the H5 WT, H5 N484A, and PBS immunizations had no significant differences in the competition with either CR6261 (Fig. 7E) or FI6v3 (Fig. 7G). The preabsorbed antisera from H5 N484A immunizations resulted in a sig-



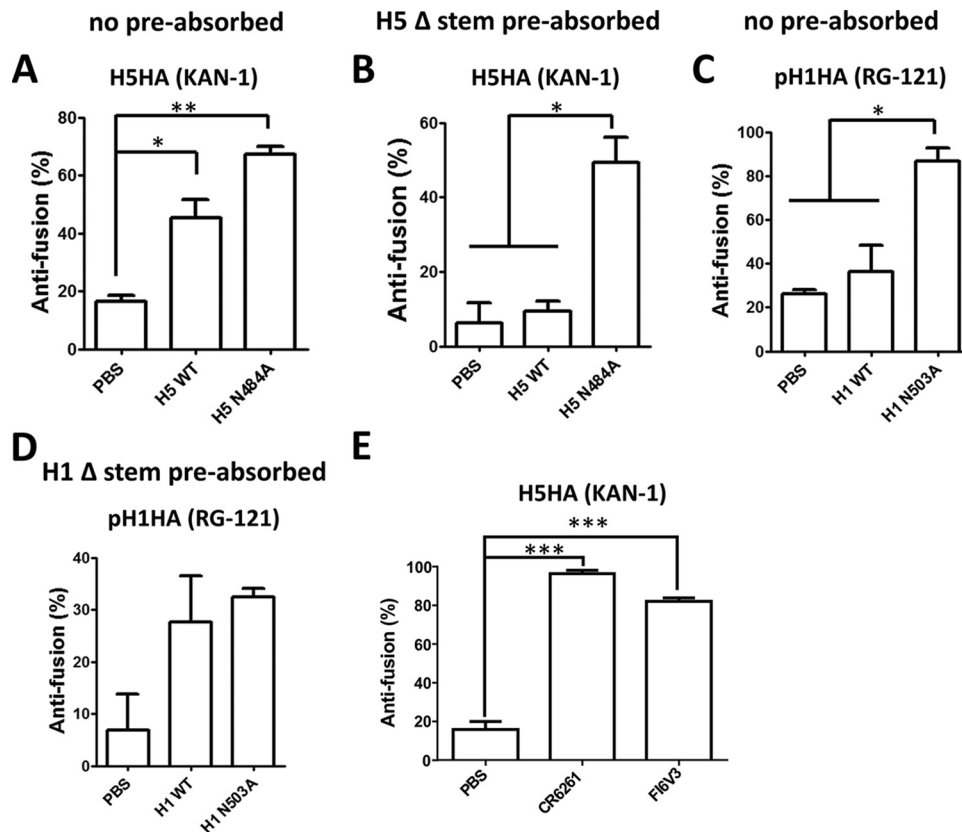


**FIG 8** Antifusion activity elicited by HA2 stem mutant protein immunization. A luciferase-based cell-cell fusion assay was used to determine antifusion activity. (A to D) Serum samples obtained from mice immunized with H5 WT and H5 N484A or H1 WT and H1 N503A were treated without preabsorption (A and C) or with H5  $\Delta$  stem protein (B) or H1  $\Delta$  stem protein (D) preabsorption and measured for antifusion activity. (E) Antifusion activity was also measured with two stem-specific bNAbs, CR6261 and FI6V3, at 10  $\mu$ g/ml. Statistical analysis consisted of one-way ANOVA. \*,  $P < 0.05$ ; \*\*,  $P < 0.01$ ; \*\*\*,  $P < 0.001$ .

nificant reduction due to the competition with either FI6V3 (Fig. 7F) or FI6V3 (Fig. 7H). No significant differences in the competition bindings were observed in H1 WT-, H1 N503A-, and PBS-immunized antisera with either CR6261 or FI6V3 competition (Fig. 7I to L). Only immunization with unmasking of the HA2 stem N-glycans of H5HA (H5 N484A) induced more CR6261-like and FI6V3-like antibodies.

**Fusion inhibition activity elicited by HA2 stem mutant protein immunization.** To examine fusion inhibition activity in antisera, we used luciferase reporter gene-based fusion assays to quantitate HA-induced pH-dependent cell-cell fusion levels as previously described (32, 33). H5 WT-, H5 N484A-, H1 WT-, and H1 N503A-immunized sera were reacted with firefly and *Renilla* luciferase reporter gene-transfected 293T cells for 48 h at 37°C and examined for cell-cell fusion activity induced by H5HA [A/Thailand/1(KAN-1)/2004, KAN-1] or pH1HA [A/California/07/2009, RG-121]. Our data indicate that the H5 N484A-immunized sera without or with H5  $\Delta$  stem protein preabsorption exhibited significantly enhanced fusion inhibition activity compared to that for the H5 WT- and PBS-immunized groups (Fig. 8A and B). Only the sera from the H1 N503A-immunized group without preabsorption induced higher antifusion activity. No increase of the fusion inhibition activity was found for the antisera with H1  $\Delta$  stem protein preabsorption compared to the H1 WT- and PBS-immunized groups (Fig. 8C and D). The cell

fusion activity was also completely blocked by two stem-specific bNAbs, CR6261 and FI6V3 (Fig. 8E).

**Stem helix A peptide-stimulated B cell subsets elicited by HA2 stem mutant protein immunization.** To measure stem helix A epitope-specific B cells following rHA protein immunizations, splenocytes were collected from mice in each immunization group and reacted with H1 or H5 helix A peptides for 48 h. HA stem<sub>518–526</sub> peptides (with the same H1-H5 sequence) served as controls. ELISPOT and flow cytometry assays were used to measure numbers of antibody (IgG)-secreting B cells (ASCs), IgG1<sup>+</sup> CD38<sup>−</sup> GC B cells, and IgG1<sup>+</sup> CD38<sup>+</sup> memory B cells. The results indicate that only the H5 N484A immunization group, and not the H1 N503A immunization group, exhibited increased numbers of ASCs, GC B cells, and memory B cells (Fig. 9). No differences were observed among any numbers of B cells elicited by the H5 WT/H5 N484A or H1 WT/H1 N503A immunization groups when control stem<sub>518–526</sub> peptides were used for B cell stimulation. Only the H5 N484A mutant protein immunization enhanced the helix A epitope-specific B cell subsets in splenocytes.

**Protective immunity elicited by HA2 stem mutant protein immunization.** To investigate protection levels elicited by HA2 stem mutant proteins, immunized mice were challenged with 10-fold 50% murine lethal doses (MLD<sub>50</sub>) of H5N1 (RG-14) or pH1N1 (CA/09) virus to assess protective immunity. Our results indicate that the H5 N484A group had a significantly increased

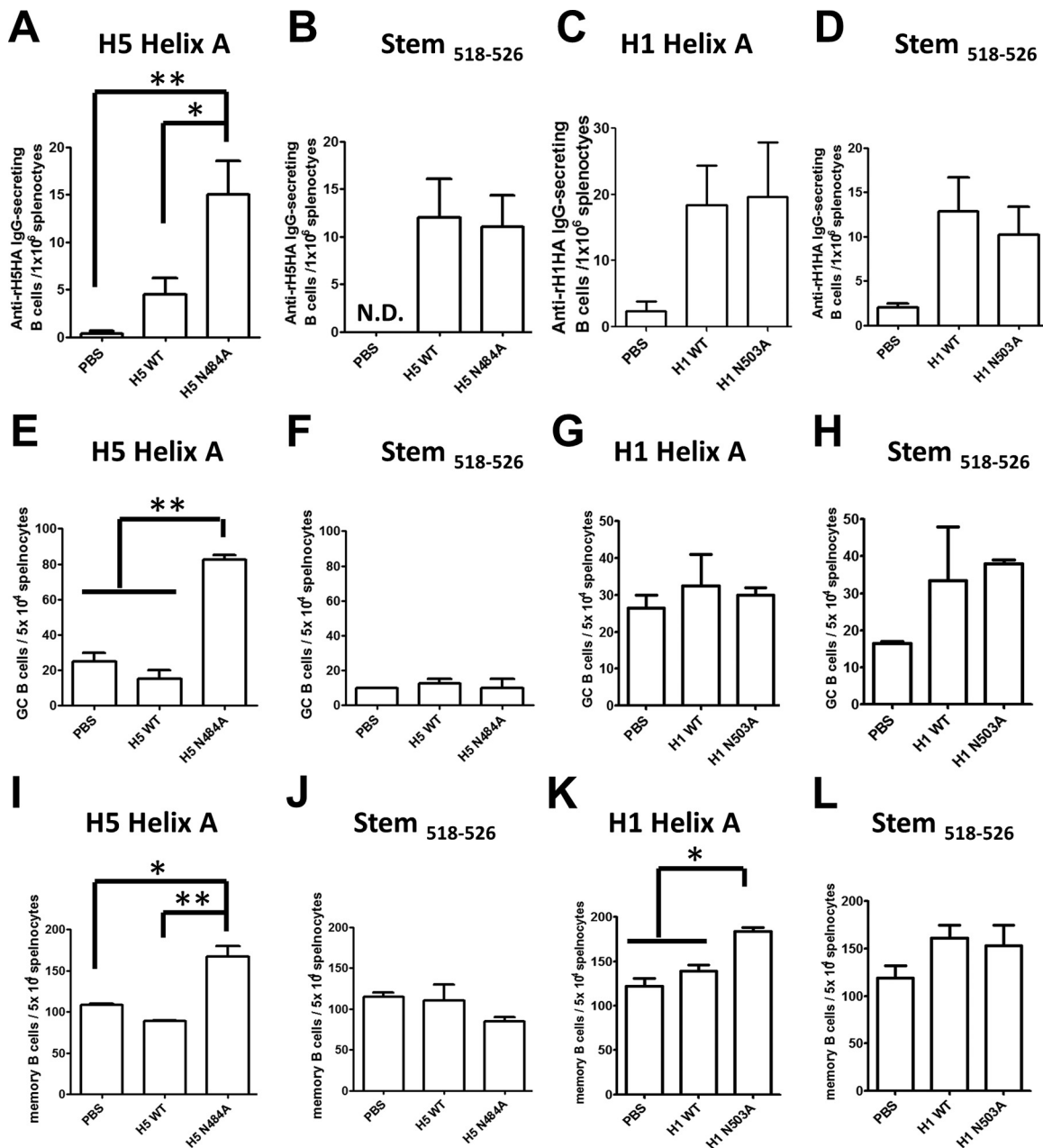


**FIG 9** Detection of ASC, GC B cell, and memory B cell subsets in splenocytes induced by rH5HA and rH1HA HA2 stem mutants. Splenocytes collected from mice immunized with H5 WT, H5 N484A, H1 WT, or H1 N503A were stimulated with helix A peptides (H5 or H1) or unrelated stem<sub>518-526</sub> Peptides (control) and held for 48 h at 37°C. (A to D) ELISPOT assays were used to measure ASCs. (E to L) Flow cytometry was used to measure the GC B cell subset (E to H) and memory B cell subset (I to L). Data are expressed as the mean  $\pm$  SD. Statistical analysis consisted of two-tailed Student *t* tests for two-group comparisons between WT and mutants. \*,  $P < 0.05$ ; \*\*,  $P < 0.01$ .

survival rate to 80% following homologous H5N1 virus challenges, compared to 40% for the H5 WT group and 0% for the PBS group (Fig. 10A). The corresponding body weight losses were recovered by the H5 WT- and H5 N484A-immunized groups but not by the PBS-immunized group (Fig. 10B). The survival rate of the H5 N484A group decreased to 20% survival (Fig. 10C) with the recovery of body weight loss following the heterosubtypic pH1N1 challenges (Fig. 10D). In contrast, the H1 N503A and WT groups all had complete protection following the homologous

pH1N1 virus challenges but no protection against the heterosubtypic H5N1 virus challenges.

## DISCUSSION

Many attempts to work on universal influenza vaccines are focusing on highly conserved HA stem regions. In this study, data from immunizations with a series of rHA mutant proteins with deleted N-linked glycosylation sites in the globular head, HA1 stem, and HA2 stem regions indicate that the elicitation of more potent neu-

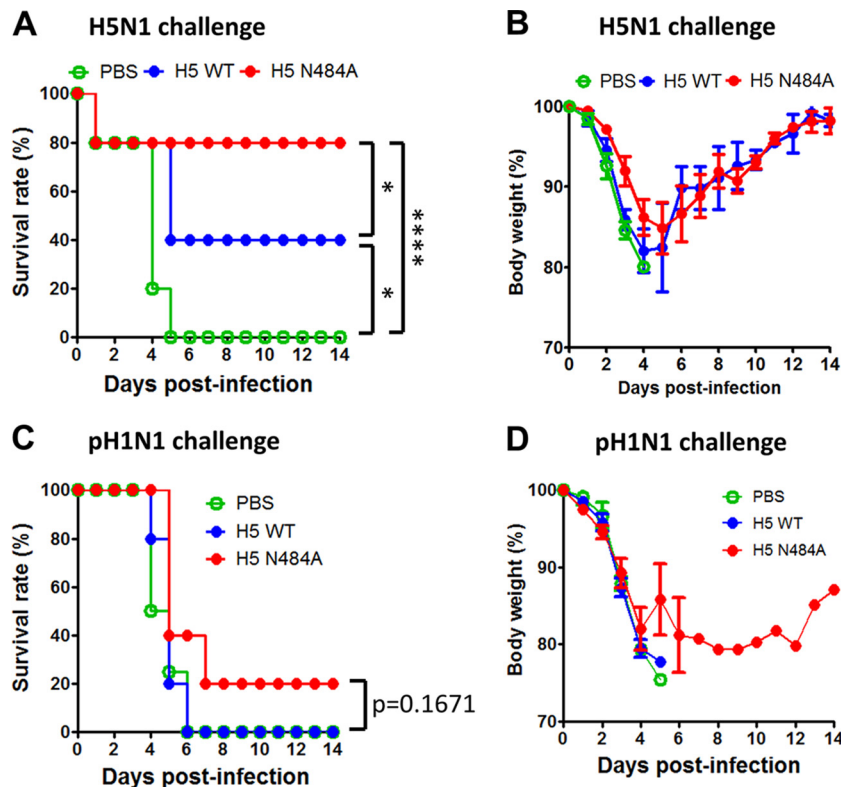


**FIG 10** Protective immunity conferred by rH5HA and rH1HA HA2 stem mutant protein vaccination against homologous and heterosubtypic viral challenges. Groups of mice (5 per group) immunized with PBS, H5 WT, or H5 N484A were intranasally challenged with 10-fold the MLD<sub>50</sub> of H5N1 (NIBRG-14 [RG-14]) or pH1N1 (A/California/07/2009) virus at 3 weeks after their second inoculations. Shown are survival curves (A and C) and body weight loss (B and D) following homologous pH1N1 or H5N1 challenges. Survival rates and body weights were recorded daily for 14 days. Body weight loss of greater than 25% was used as an endpoint. The survival curves among the PBS-, H5 WT-, and H5N484A-immunized groups were analyzed using the Mantel-Cox log rank test followed by pairwise comparison using the Gehan-Breslow-Wilcoxon test. \*,  $P < 0.05$ ; \*\*\*\*,  $< 0.0001$ . These experiments were repeated more than once, and the results were reproducible.

tralizing antibodies against different influenza A virus strains occurred only following the unmasking of HA2 stem N-glycans. Immunization using HA2 stem mutant proteins of the H5N1 KAN-1 strain induced significantly higher titers against the homologous H5N1 KAN-1 strain, the heterologous H5N1 Indonesia strain, and the heterosubtypic H3N2 Udorn strain. Immunization using HA2 stem mutant proteins of the pH1N1 Texas strain resulted in higher neutralizing antibody titers against the homologous pH1N1 California strain and the heterosubtypic H3N2 Udorn strain (Fig. 6). However, immunizations using the globular head mutant proteins H5 N154A, H5 N165A, H5 N286A, H1 N109A, H1 N298A, and H1 N309A elicited neutralization titers with only the same or lower IC<sub>50</sub> values as with the control H5 WT and H1 WT proteins (Fig. 6). These results are in agreement with a recent study using mutant viruses with the loss of N-glycans in the globular head region with lowered immunogenicity in mice (12). In contrast, others have reported that removal of N-glycans in the globular head region resulted in increased virulence in mice (35, 36) and improved live-attenuated vaccine immunity in ferrets (37). According to our alignment results for H1HA and H5HA sequences from position 1918 to 2016 (<http://www.ncbi.nlm.nih.gov/genomes/FLU/Database/nph-select.cgi>), most of the isolates of H1HA and H5HA share the same N-glycan (NGTY) modifications on the HA2 stem region (N503 for H1HA and N484 for H5HA).

Mapping the immune sera for stem-binding antibodies was conducted by preabsorbing non-stem-specific antibodies with H5  $\Delta$  stem or H1  $\Delta$  stem proteins before measuring stem-specific antibodies bound to rH5HA or rH1HA proteins in ELISAs. Our results indicate that unmasking the HA stem N-glycans did not increase the amounts of total stem-binding antibodies (Fig. 7C and D). However, the results from the competition assay using two stem-specific bNAbs showed that unmasking the HA2 stem N-glycans for the H5 N484A mutant led to more CR6261-like and FI6v3-like antibodies in antisera (Fig. 7F, H). The binding sites in the HA2 stem for CR6261 and FI6v3 are not completely overlapped (25), for the interaction of FI6v3 with the hydrophobic groove on HA is mediated by long HCDR3 (heavy-chain constant domain region 3) and LCDR1 (light-chain constant domain region 1), whereas CR6261 interacted with all of three HCDRs (CDR1 to CDR3). Both antibodies (FI6v3 and CR6261) make contacts with Trp<sup>21</sup>, mainly through a phenylalanine side chain: Phe<sup>100D</sup> on FI6v3 and Phe<sup>54</sup> on CR6261 (25). Both CR6261 and FI6v3 bNAbs demonstrated complete inhibition in the cell fusion assay (Fig. 8E). The increased CR6261-like and FI6v3-like antibodies in antisera raised from the H5 N484A mutant (Fig. 7E and H) also correlated with the increase of fusion inhibition activity in both nonabsorbed and H5  $\Delta$  stem-preabsorbed sera (Fig. 8A and B). However, the H1 N503A mutant did not show increased CR6261-like and FI6v3-like antibodies (Fig. 7I to L) and increased



the fusion inhibition activity only in nonabsorbed (Fig. 8C) and not in H1  $\Delta$  stem-preabsorbed (Fig. 8D) sera. The inconsistency for the H1 N503A mutant sera may reflect a significant fraction of serum antibodies that do not overlap where the N-glycan has been introduced in the midstem region of the H1  $\Delta$  stem construct, since the nonabsorbed H1 N503A sera had a significant higher antifusion activity.

Since the helix A epitope in the F subdomain of the HA2 stem region appears to be the target for several stem-specific bNAbs (25), we measured numbers of ASCs, GC B cells, and memory B cells that are specific to HA2 stem helix A epitopes in immunized mice. The numbers of helix A-stimulated ASCs, GC B cells, and memory B cell subsets in splenocytes were significantly higher following H5 N484A immunization with H5 helix A stimulation (Fig. 9E and I). All of these results suggest that unmasking the HA2 stem N-glycans particularly for H5 N484A mutant immunization can refocus B antibody responses to the helix A epitope for inducing more CR6261-like/FI6v3-like and fusion inhibition antibodies.

Unmasking the HA2 stem N-glycans of H5HA mutant proteins shows a significant improvement in the protection against homologous virus challenges (i.e., a 40% increased survival rate) but to a less degree for the protection against heterosubtypic pH1N1 virus challenges (i.e., a 20% increased survival rate) (Fig. 10). The improved protective levels were not found for H1 N503A mutant immunization against the heterologous H5N1 challenges even though complete protection was observed following the homologous pH1N1 virus challenges. It is likely that only unmasking of the membrane-proximal glycan works in eliciting a protective response in context of H5HA but not H1HA, since the viral membrane-distal ends to the C-terminal anchor region are different in the H5HA and H1HA 3D structures (Fig. 1). Furthermore, the improved protection by H5 N484A mutant immunization but not by H1 N503A mutant immunization was correlated with increased titers of virus-neutralizing antibodies, more of the stem-specific CR6261-like and FI6v3-like antibodies (Fig. 7F and H), and enhanced levels of fusion inhibition antibodies (Fig. 8A and B). However, the quantities of total stem-binding antibodies obtained by H5 WT and H5 N484A mutant immunizations were around the same (Fig. 7C). It is possible that the heterosubtypic cross protection is more associated with the total stem-binding antibodies, and not only restricted to the stem-specific CR6261-like and FI6v3-like antibodies, as recently reported for Fc-Fc $\gamma$ R engagements but not through their binding epitope(s) (38, 39). Also, the presence of the immune-dominant globular head region may dilute the outcomes of the stem glycan removal strategy in terms of heterosubtypic protection. Therefore, this vaccine design still needs further optimization to include other strategies such as the combination with globular head glycan masking, as we and others previously reported (19–21). All of these results can provide useful information for developing more effective influenza vaccines.

## ACKNOWLEDGMENTS

We thank Ming-Hsi Huang for providing PELC adjuvant, Ken Ishii for providing CpG adjuvant, Yoshiharu Matsuura for providing the pCAGT7pol and pT7EMCVLuc plasmids for fusion assay, and Ya-Lin Yang for performing the CR6261 and FI6v3 fusion inhibition assay.

## FUNDING INFORMATION

This work, including the efforts of Suh-Chin Wu, was funded by Ministry of Science and Technology, Taiwan (MOST) (MOST105-2321-B-007-005 and MOST105-2321-B-007-006). This work, including the efforts of Suh-Chin Wu, was funded by National Tsing Hua University (NTHU) (105N742CV8).

The funders had no role in the study design, data collection and analysis, decision to publish, or manuscript preparation.

## REFERENCES

1. Wohlbold TJ, Krammer F. 2014. In the shadow of hemagglutinin: a growing interest in influenza viral neuraminidase and its role as a vaccine antigen. *Viruses* 6:2465–2494. <http://dx.doi.org/10.3390/v6062465>.
2. Tong S, Zhu X, Li Y, Shi M, Zhang J, Bourgeois M, Yang H, Chen X, Recuenco S, Gomez J, Chen LM, Johnson A, Tao Y, Dreyfus C, Yu W, McBride R, Carney PJ, Gilbert AT, Chang J, Guo Z, Davis CT, Paulson JC, Stevens J, Rupprecht CE, Holmes EC, Wilson IA, Donis RO. 2013. New world bats harbor diverse influenza A viruses. *PLoS Pathog* 9:e1003657. <http://dx.doi.org/10.1371/journal.ppat.1003657>.
3. Gamblin SJ, Skehel JJ. 2010. Influenza hemagglutinin and neuraminidase membrane glycoproteins. *J Biol Chem* 285:28403–28409. <http://dx.doi.org/10.1074/jbc.R110.129809>.
4. Trock SC, Burke SA, Cox NJ. 2015. Development of framework for assessing influenza virus pandemic risk. *Emerg Infect Dis* 21:1372–1378. <http://dx.doi.org/10.3201/eid2108.141086>.
5. Krammer F, Palese P. 2015. Advances in the development of influenza virus vaccines. *Nat Rev Drug Discov* 14:167–182. <http://dx.doi.org/10.1038/nrd4529>.
6. Skehel JJ, Wiley DC. 2000. Receptor binding and membrane fusion in virus entry: the influenza hemagglutinin. *Annu Rev Biochem* 69:531–569. <http://dx.doi.org/10.1146/annurev.biochem.69.1.531>.
7. Das SR, Puigbo P, Hensley SE, Hurt DE, Bennis JR, Yewdell JW. 2010. Glycosylation focuses sequence variation in the influenza A virus H1 hemagglutinin globular domain. *PLoS Pathog* 6:e1001211. <http://dx.doi.org/10.1371/journal.ppat.1001211>.
8. Medina RA, Stertz S, Manicassamy B, Zimmermann P, Sun X, Albrecht RA, Uusi-Kerttula H, Zagordi O, Belshe RB, Frey SE, Tumpey TM, Garcia-Sastre A. 2013. Glycosylations in the globular head of the hemagglutinin protein modulate the virulence and antigenic properties of the H1N1 influenza viruses. *Sci Transl Med* 5:187ra170.
9. Krammer F, Palese P. 2013. Influenza virus hemagglutinin stalk-based antibodies and vaccines. *Curr Opin Virol* 3:521–530. <http://dx.doi.org/10.1016/j.coviro.2013.07.007>.
10. Steel J, Lowen AC, Wang TT, Yondola M, Gao Q, Haye K, Garcia-Sastre A, Palese P. 2010. Influenza virus vaccine based on the conserved hemagglutinin stalk domain. *mBio* 1:e00018-10. <http://dx.doi.org/10.1128/mBio.00018-10>.
11. Wagner R, Heuer D, Wolff T, Herwig A, Klenk HD. 2002. N-glycans attached to the stem domain of haemagglutinin efficiently regulate influenza A virus replication. *J Gen Virol* 83:601–609. <http://dx.doi.org/10.1099/0022-1317-83-3-601>.
12. Zhang X, Chen S, Yang D, Wang X, Zhu J, Peng D, Liu X. 2015. Role of stem glycans attached to haemagglutinin in the biological characteristics of H5N1 avian influenza virus. *J Gen Virol* 96:1248–1257. <http://dx.doi.org/10.1099/vir.0.000082>.
13. Khanna M, Sharma S, Kumar B, Rajput R. 2014. Protective immunity based on the conserved hemagglutinin stalk domain and its prospects for universal influenza vaccine development. *Biomed Res Int* 2014:546274. <http://dx.doi.org/10.1155/2014/546274>.
14. Laursen NS, Wilson IA. 2013. Broadly neutralizing antibodies against influenza viruses. *Antiviral Res* 98:476–483. <http://dx.doi.org/10.1016/j.antiviral.2013.03.021>.
15. Krammer F, Hai R, Yondola M, Tan GS, Leyva-Grado VH, Ryder AB, Miller MS, Rose JK, Palese P, Garcia-Sastre A, Albrecht RA. 2014. Assessment of influenza virus hemagglutinin stalk-based immunity in ferrets. *J Virol* 88:3432–3442. <http://dx.doi.org/10.1128/JVI.03004-13>.
16. Krammer F, Pica N, Hai R, Margine I, Palese P. 2013. Chimeric hemagglutinin influenza virus vaccine constructs elicit broadly protective stalk-specific antibodies. *J Virol* 87:6542–6550. <http://dx.doi.org/10.1128/JVI.00641-13>.
17. Impagliazzo A, Milder F, Kuipers H, Wagner M, Zhu X, Hoffman RM,

- van Meersbergen R, Huizingh J, Wanningen P, Verspuij J, de Man M, Ding Z, Apetri A, Kukrer B, Sneekes-Vriese E, Tomkiewicz D, Laursen NS, Lee PS, Zakrzewska A, Dekking L, Tolboom J, Tetters L, van Meerten S, Yu W, Koudstaal W, Goudsmit J, Ward AB, Meijberg W, Wilson IA, Radosevic K. 2015. A stable trimeric influenza hemagglutinin stem as a broadly protective immunogen. *Science* 349:1301–1306. <http://dx.doi.org/10.1126/science.aac7263>.
18. Yassine HM, Boyington JC, McTamney PM, Wei CJ, Kanekiyo M, Kong WP, Gallagher JR, Wang L, Zhang Y, Joyce MG, Lingwood D, Moin SM, Andersen H, Okuno Y, Rao SS, Harris AK, Kwong PD, Mascola JR, Nabel GJ, Graham BS. 2015. Hemagglutinin-stem nanoparticles generate heterosubtypic influenza protection. *Nat Med* 21:1065–1070. <http://dx.doi.org/10.1038/nm.3927>.
19. Lin SC, Lin YF, Chong P, Wu SC. 2012. Broader neutralizing antibodies against H5N1 viruses using prime-boost immunization of hyperglycosylated hemagglutinin DNA and virus-like particles. *PLoS One* 7:e39075. <http://dx.doi.org/10.1371/journal.pone.0039075>.
20. Lin SC, Liu WC, Jan JT, Wu SC. 2014. Glycan masking of hemagglutinin for adenovirus vector and recombinant protein immunizations elicits broadly neutralizing antibodies against H5N1 avian influenza viruses. *PLoS One* 9:e92822. <http://dx.doi.org/10.1371/journal.pone.0092822>.
21. Eggink D, Goff PH, Palese P. 2014. Guiding the immune response against influenza virus hemagglutinin toward the conserved stalk domain by hyperglycosylation of the globular head domain. *J Virol* 88:699–704. <http://dx.doi.org/10.1128/JVI.02608-13>.
22. Margine I, Krammer F, Hai R, Heaton NS, Tan GS, Andrews SA, Runstadler JA, Wilson PC, Albrecht RA, Garcia-Sastre A, Palese P. 2013. Hemagglutinin stalk-based universal vaccine constructs protect against group 2 influenza A viruses. *J Virol* 87:10435–10446. <http://dx.doi.org/10.1128/JVI.01715-13>.
23. Ekiert DC, Bhabha G, Elsliger MA, Friesen RH, Jongeneelen M, Thorsby M, Goudsmit J, Wilson IA. 2009. Antibody recognition of a highly conserved influenza virus epitope. *Science* 324:246–251. <http://dx.doi.org/10.1126/science.1171491>.
24. Sui J, Hwang WC, Perez S, Wei G, Aird D, Chen LM, Santelli E, Stec B, Cadwell G, Ali M, Wan H, Murakami A, Yammanuru A, Han T, Cox NJ, Bankston LA, Donis RO, Liddington RC, Marasco WA. 2009. Structural and functional bases for broad-spectrum neutralization of avian and human influenza A viruses. *Nat Struct Mol Biol* 16:265–273. <http://dx.doi.org/10.1038/nsmb.1566>.
25. Corti D, Voss J, Gambin SJ, Codoni G, Macagno A, Jarrossay D, Vachieri SG, Pinna D, Minola A, Vanzetta F, Silacci C, Fernandez-Rodriguez BM, Agatic G, Bianchi S, Giacchetto-Sasselli I, Calder L, Sallusto F, Collins P, Haire LF, Temperton N, Langedijk JP, Skehel JJ, Lanzavecchia A. 2011. A neutralizing antibody selected from plasma cells that binds to group 1 and group 2 influenza A hemagglutinins. *Science* 333:850–856. <http://dx.doi.org/10.1126/science.1205669>.
26. Bullough PA, Hughson FM, Skehel JJ, Wiley DC. 1994. Structure of influenza haemagglutinin at the pH of membrane fusion. *Nature* 371:37–43. <http://dx.doi.org/10.1038/371037a0>.
27. Lingwood D, McTamney PM, Yassine HM, Whittle JR, Guo X, Boyington JC, Wei CJ, Nabel GJ. 2012. Structural and genetic basis for development of broadly neutralizing influenza antibodies. *Nature* 489:566–570. <http://dx.doi.org/10.1038/nature11371>.
28. Pappas L, Foglierini M, Piccoli L, Kallewaard NL, Turrini F, Silacci C, Fernandez-Rodriguez B, Agatic G, Giacchetto-Sasselli I, Pellicciotta G, Sallusto F, Zhu Q, Vicenzi E, Corti D, Lanzavecchia A. 2014. Rapid development of broadly influenza neutralizing antibodies through redundant mutations. *Nature* 516:418–422. <http://dx.doi.org/10.1038/nature13764>.
29. Tung CP, Chen IC, Yu CM, Peng HP, Jian JW, Ma SH, Lee YC, Jan JT, Yang AS. 2015. Discovering neutralizing antibodies targeting the stem epitope of H1N1 influenza hemagglutinin with synthetic phage-displayed antibody libraries. *Sci Rep* 5:15053. <http://dx.doi.org/10.1038/srep15053>.
30. Liu WC, Lin SC, Yu YL, Chu CL, Wu SC. 2010. Dendritic cell activation by recombinant hemagglutinin proteins of H1N1 and H5N1 influenza A viruses. *J Virol* 84:12011–12017. <http://dx.doi.org/10.1128/JVI.01316-10>.
31. Wei CJ, Boyington JC, McTamney PM, Kong WP, Pearce MB, Xu L, Andersen H, Rao S, Tumpey TM, Yang ZY, Nabel GJ. 2010. Induction of broadly neutralizing H1N1 influenza antibodies by vaccination. *Science* 329:1060–1064. <http://dx.doi.org/10.1126/science.1192517>.
32. Su Y, Yang H, Zhang B, Qi X, Tien P. 2008. A dual reporter gene based system to quantitate the cell fusion of avian influenza virus H5N1. *Bio-technol Lett* 30:73–79.
33. Takikawa S, Ishii K, Aizaki H, Suzuki T, Asakura H, Matsuura Y, Miyamura T. 2000. Cell fusion activity of hepatitis C virus envelope proteins. *J Virol* 74:5066–5074. <http://dx.doi.org/10.1128/JVI.74.11.5066-5074.2000>.
34. Aiba Y, Kometani K, Hamadate M, Moriyama S, Sakaue-Sawano A, Tomura M, Luche H, Fehling HJ, Casellas R, Kanagawa O, Miyawaki A, Kurosaki T. 2010. Preferential localization of IgG memory B cells adjacent to contracted germinal centers. *Proc Natl Acad Sci U S A* 107:12192–12197. <http://dx.doi.org/10.1073/pnas.1005443107>.
35. Suptawiwat O, Boonarkart C, Chakritbudsabong W, Uiprasertkul M, Puthavathana P, Wiriyarat W, Auewarakul P. 2015. The N-linked glycosylation site at position 158 on the head of hemagglutinin and the virulence of H5N1 avian influenza virus in mice. *Arch Virol* 160:409–415. <http://dx.doi.org/10.1007/s00705-014-2306-x>.
36. Tate MD, Brooks AG, Reading PC. 2011. Specific sites of N-linked glycosylation on the hemagglutinin of H1N1 subtype influenza A virus determine sensitivity to inhibitors of the innate immune system and virulence in mice. *J Immunol* 187:1884–1894. <http://dx.doi.org/10.4049/jimmunol.1100295>.
37. Wang W, Lu B, Zhou H, Suguitan AL, Jr, Cheng X, Subbarao K, Kemble G, Jin H. 2010. Glycosylation at 158N of the hemagglutinin protein and receptor binding specificity synergistically affect the antigenicity and immunogenicity of a live attenuated H5N1 A/Vietnam/1203/2004 vaccine virus in ferrets. *J Virol* 84:6570–6577. <http://dx.doi.org/10.1128/JVI.00221-10>.
38. DiLillo DJ, Tan GS, Palese P, Ravetch JV. 2014. Broadly neutralizing hemagglutinin stalk-specific antibodies require FcγR interactions for protection against influenza virus in vivo. *Nat Med* 20:143–151. <http://dx.doi.org/10.1038/nm.3443>.
39. DiLillo DJ, Palese P, Wilson PC, Ravetch JV. 2016. Broadly neutralizing anti-influenza antibodies require Fc receptor engagement for in vivo protection. *J Clin Invest* 126:605–610. <http://dx.doi.org/10.1172/JCI84428>.